Green's function for δ-function potentials with a hard core: Application to multiphoton photodetachment of negative halogen ions

S. H. Patil
Department of Physics, Indian Institute of Technology, Bombay 400 076, India
(Received 30 September 1991; revised manuscript received 1 June 1992)

We develop a simple Green's function for δ-function potentials with a hard core, and use it to calculate polarizabilities of negative halogen ions and multiphoton-detachment cross sections for these ions. The predictions indicate an influence of a resonance for two- and three-photon cross sections, and yield approximately universal relative amplitudes as functions of a scaled electron energy.

PACS number(s): 32.80.Fb, 32.80.Rm, 35.10.Di

I. INTRODUCTION

Green's functions are of great importance in the understanding of many physical processes. In particular, they are useful in evaluating amplitudes for multiphoton ionization of atoms and ions. Here we obtain Green's function for a model potential consisting of some δ functions and a hard core, and use it to analyze the cross sections for multiphoton photodetachment of negative halogen ions.

A. A brief review

It was quite some time ago that the first calculations [1,2] of the amplitude for two-photon detachment of negative ions were carried out. In these calculations, major approximations were made for either the energy denominator [1] or for the intermediate and final-state wave functions [2]. Soon after this, measurements [3] were made for the two-photon detachment of I^-. Some time later, Robinson and Geltman [4] carried out detailed calculations for the detachment cross sections using a model, central potential for the electron. The results were in agreement with the experimental results for I^-. Recently, there has been a sudden spurt of activity in the field of photodetachment of ions, and new experimental results have been obtained. Now we have some information [5–9] about multiphoton detachment of F^-, Cl^-, Br^-, and I^-. On the theoretical side, detailed calculations have been carried out [10–12] for photodetachment processes using different approximations, in particular Hartree-Fock approximation for some ions. However, there is a considerable variation in the predictions of different models and the agreement between the theoretical predictions and the experimental observations is not always satisfactory. Therefore there is a need for further theoretical investigation of the processes.

Green's-function methods are widely used in the analysis of multiphoton detachment of atoms and ions. Specifically, Coulombic Green's functions [13] are used directly or indirectly to carry out the infinite summations for multiphoton detachment of atoms [14]. For processes involving negative ions, the infinite summation has been carried out [4,10] by solving the inhomogeneous equation for the perturbed part of the wave function. The potential used in these calculations is based on the Hartree-Fock approximation, or some central field with a polarization term.

B. An outline of our work

Our work is based on the idea that an electron in a negative halogen ion sees an attractive potential when it is far away from the remaining atom, mainly due to the induced dipole moment, and experiences a strong, exchange, repulsive force when it is close to the atom. We approximate this by some δ-function potential with a repulsive hard core. We then deduce the exact, energy-dependent Green's function for this potential. This Green's function is then used to evaluate the dipolar polarizabilities of the negative halogen ions, and the cross sections for the two-, three-, and four-photon detachment of negative ions. The predictions are found to be in good agreement with the experimental results. They also indicate an influence of a resonance for the two- and three-photon detachment of negative halogen ions, and essentially universal ratios for different amplitudes as functions of a scaled electron energy.

II. GREEN'S FUNCTION FOR δ-FUNCTION POTENTIALS WITH A HARD CORE

Consider the Green's function for the potential

$$V(r)=V_0(r)+V_1(r)\ , \tag{2.1}$$

where

$$V_0(r)=\begin{cases}0 & \text{for } r>R\\ \infty & \text{for } r\le R\end{cases}\ , \tag{2.2}$$

$$V_1(r)=-\sum_i Z_i\delta(r-a_i),\quad a_i>R\ . \tag{2.3}$$

The Green's function satisfies the equation

$$\left[-\frac{\hbar^2}{2m}\nabla^2+V(r)-E\right]G(\mathbf{r},\mathbf{r}')=\delta(\mathbf{r}-\mathbf{r}')\ . \tag{2.4}$$

With the usual partial-wave projection we have

$$G(\mathbf{r},\mathbf{r}')=\frac{1}{4\pi}\sum_{l=0}^{\infty}(2l+1)g_l(r,r')P_l(\hat{\mathbf{r}}\cdot\hat{\mathbf{r}}') , \tag{2.5}$$

where $g_l(r,r')$ satisfies the equation

$$-\frac{\hbar^2}{2m}\left[\frac{1}{r^2}\frac{\partial}{\partial r}r^2\frac{\partial}{\partial r}-\frac{l(l+1)}{r^2}\right]g_l(r,r') +[V(r)-E]g_l(r,r')=\frac{1}{r^2}\delta(r-r') . \tag{2.6}$$

We first solve the equation with only the hard-core potential and then obtain the Green's function for the full potential.

A. Green's function with only the hard core

The Green's function with only the hard core, $g_l^{(0)}(r,r')$, satisfies the equation.

$$\left[\frac{1}{r^2}\frac{\partial}{\partial r}r^2\frac{\partial}{\partial r}-\frac{l(l+1)}{r^2}+k^2\right]g_l^{(0)}(k,r,r') =-\frac{2m}{\hbar^2 r^2}\delta(r-r') , \tag{2.7}$$

$$k^2=\frac{2mE}{\hbar^2} ,$$

with the boundary condition

$$g_l^{(0)}(k,R,r')=0 , \qquad g_l^{(0)}(k,r,r')\sim\frac{1}{r}e^{ikr} \text{ for } r\to\infty . \tag{2.8}$$

Taking appropriate combinations of spherical Bessel functions, the solutions are found to be

$$g_l^{(0)}(k,r,r')=\left[\frac{2mik}{\hbar^2}\right] \times\frac{n_l(kR)j_l(kr_<)-j_l(kR)n_l(kr_<)}{n_l(kR)-ij_l(kR)} \times h_l^{(1)}(kr_>) , \tag{2.9}$$

where j_l and n_l are the spherical Bessel functions of the first and second kind,

$$h_l^{(1)}(z)=j_l(z)+in_l(z) , \tag{2.10}$$

and $r_<=\min(r,r')$, $r_>=\max(r,r')$.

B. The perturbed Green's function

The Green's function with both the hard core and the δ-function potentials satisfies the integral equation

$$g_l(k,r,r')=g_l^{(0)}(k,r,r) -\int g_l^{(0)}(k,r,r'')V_1(r'') \times g_l(k,r'',r')r''^2dr'' . \tag{2.11}$$

Substituting the expression for $V_1(r)$ in Eq. (2.3), we get

$$g_l(k,r,r')=g_l^{(0)}(k,r,r') +\sum_i Z_i g_l^{(0)}(k,r,a_i)g_l(k,a_i,r')a_i^2 . \tag{2.12}$$

With $r=a_j$, we get a set of equations

$$g_l(k,a_j,r')=g_l^{(0)}(k,a_j,r') +\sum_i Z_i g_l^{(0)}(k,a_j,a_i)a_i^2 g_l(k,a_i,r') . \tag{2.13}$$

Solving for $g_l(k,a_j,r')$, one finally gets

$$g_l(k,r,r')=g_l^{(0)}(k,r,r') +\sum_i Z_i g_l^{(0)}(k,r,a_i)a_i^2 \times\sum_j[(1-N)^{-1}]_{ij}g_l^{(0)}(k,a_j,r') , \tag{2.14}$$

where $g_l^{(0)}$ are given in Eq. (2.9) and N is the matrix with elements

$$N_{ij}=g_l^{(0)}(k,a_i,a_j)Z_j a_j^2 . \tag{2.15}$$

C. Green's function for negative halogen ions

The last electron in a negative halogen atom is loosely bound. It sees an attractive potential due to the induced moments, mainly dipolar and quadrupolar moments and experiences a strong, exchange, repulsive force when it is close to the atom. We approximate this interaction by a hard-core potential with only one δ function. This leads to Green's function

$$g_l(k,r,r')=g_l^{(0)}(k,r,r') +Z_l g_l^{(0)}(k,r,a)a^2 g_l^{(0)}(k,a,r') \times\frac{1}{1-g_l^{(0)}(k,a,a)Z_l a^2} , \tag{2.16}$$

where the strength Z_l of the δ function will in general depend on l.

III. WAVE FUNCTIONS FOR BOUND AND POSITIVE-ENERGY STATES

For evaluating the transition amplitudes, one needs the wave functions for the initial and final states. These are obtained by considering an electron in the presence of a δ-function potential with a hard core.

A. Bound-state wave function

We consider the Schrödinger equation for a δ-function potential with a hard core. The bound-state wave function of the loosely bound electron in the negative halogen ion satisfies the $l=1$ partial-wave Schrödinger equation

$$\psi_b^{m_1}(\mathbf{r})=Y_1^{m_1}(\theta,\phi)\cdot\phi_b(r) , \tag{3.1}$$

$$\left[\frac{1}{r^2}\frac{\partial}{\partial r}r^2\frac{\partial}{\partial r}-\frac{2}{r^2}-b^2\right]\phi_b(r) = -\frac{2mZ_1}{\hbar^2}\delta(r-a)\phi_b(r) , \quad (3.2)$$

$$b=(2mE_b/\hbar^2)^{1/2} , \quad (3.3)$$

with the boundary condition

$$\phi_b(R)=0 , \quad (3.4)$$

where E_b is the electron affinity of the halogen atom. The solution is given by

$$\phi_b(r)=\begin{cases} A_1[h_1^{(1)}(ibr)h_1^{(2)}(ibR)-h_1^{(1)}(ibR)h_1^{(2)}(ibr)] & \text{for } r\le a \\ A_1[h_1^{(1)}(iba)h_1^{(2)}(ibR)-h_1^{(1)}(ibR)h_1^{(2)}(iba)]h_1^{(1)}(ibr)/h_1^{(1)}(iba) & \text{for } r>a , \end{cases} \quad (3.5)$$

with Z_1 and b related by the equation

$$Z_1 ba^2[h_1^{(1)}(iba)h_1^{(2)}(ibR)-h_1^{(1)}(ibR)h_1^{(2)}(iba)]h_1^{(1)}(iba) = h_1^{(1)}(ibR) , \quad (3.6)$$

where $h_1^{(1)}$ and $h_1^{(2)}$ are spherical Hankel functions of the first and second kind. Constant A_1 is determined from the normalization condition

$$\int_R^\infty [\phi_b(r)]^2 r^2 dr = 1 . \quad (3.7)$$

B. Positive-energy wave functions

The positive-energy wave functions satisfy the following partial-wave Schrödinger equation:

$$\psi_l^{m_l}(k,\mathbf{r})=Y_l^{m_l}(\theta,\phi)\phi_l(k,r) , \quad (3.8)$$

$$\left[\frac{1}{r^2}\frac{\partial}{\partial r}r^2\frac{\partial}{\partial r}-\frac{l(l+1)}{r^2}+k^2\right]\phi_l(k,r) = -\frac{2mZ_l}{\hbar^2}\delta(r-a)\phi_l(k,r) , \quad (3.9)$$

$$k=(2mE/\hbar^2)^{1/2} , \quad (3.10)$$

with the boundary condition

$$\phi_l(k,R)=0 . \quad (3.11)$$

The solutions may be written as

$$\phi_l(k,R)=B_l[n_l(kR)j_l(kr)-n_l(kr)j_l(kR)] \text{ for } r\le a = B_l[C_l j_l(kr)-D_l n_l(kr)] \text{ for } r>a , \quad (3.12)$$

with

$$C_l=n_l(kR)+\frac{2mZ_l}{\hbar^2}a^2 k n_l(ka)[n_l(kR)j_l(ka) - n_l(ka)j_l(kR)] , \quad (3.13)$$

$$D_l=j_l(kR)+\frac{2mZ_l}{\hbar^2}a^2 k j_l(ka)[n_l(kR)j_l(ka) - n_l(ka)j_l(kR)] , \quad (3.14)$$

$$B_l=k(2/\pi)^{1/2}[C_l^2+D_l^2]^{-1/2} , \quad (3.15)$$

where j_l and n_l are spherical Bessel functions of the first and second kind, and the wave functions have the normalization

$$\int \psi_{l'}^{m_{l'}*}(k',\mathbf{r})\psi_l^{m_l}(k,\mathbf{r})dV=\delta_{l,l'}\delta_{m_l m_{l'}}\delta(k-k') . \quad (3.16)$$

IV. POLARIZABILITIES AND DETACHMENT AMPLITUDES

The Green's function and the wave functions we have discussed can be used for deducing polarizabilities for negative ions and probability amplitudes for multiphoton photodetachment of these ions. We first discuss the determination of the parameters in the wave functions and in the Green's function.

A. Input parameters

The parameters of our model are the radius R of the hard core, position a, and strengths Z_l of the δ-function potentials. We determine them as follows.

We first observe that the contribution of the loosely bound electron to the susceptibility of the ion is

$$\kappa^- - \kappa = \tfrac{1}{6}\int [\phi_b(r)]^2 r^4 dr , \quad (4.1)$$

where $\phi_b(r)$ is given in Eq. (3.5). The values of κ^- and κ are given by Malli and Fraga [15] for F, Cl, Br, and their negative ions. We take slightly smaller values since the values given by Malli and Fraga [15] for inert gases are slightly larger than the experimental values. For I^- we take the average of values given in Ref. [16] and for I we take the value given by Patil [17]. Our input values for $\kappa^- - \kappa$ are given in Table I. We also have the condition in Eq. (3.6),

$$Z_1 ba^2[h_1^{(1)}(iba)h_1^{(2)}(ibR)-h_1^{(1)}(ibR)h_1^{(2)}(iba)]h_1^{(1)}(iba) = h_1^{(1)}(ibR) , \quad (4.2)$$

which is essentially the condition that the δ-function potential should produce a bound state with energy $-\hbar^2 b^2/2m$. Equations (4.1) and (4.2) may be regarded as equations for determining R and Z_1 in terms of a.

For the determination of a and Z_l, $l\neq 1$, we first observe that since the halogen atom has a vacancy in the $l=1$ shell, one expects the effective potential for the $l=1$ electron to be different from that for $l\neq 1$ electrons. One also observes that the electronic structure of the different halogen ions is similar and hence we expect a/R and

TABLE I. Input values of the electron affinity E_b for the halogen atom, difference $\kappa^- - \kappa$ in the susceptibilities of the negative ion and the neutral atom, dipolar polarizability α of the neutral atom, all in atomic units, the ratio of a/R as given in Eq. (4.5), and the ratio Z/Z_1 as given in Eq. (4.6), Z_1 and Z being the strengths of the δ-function potential for the $l=1$ and $l\neq 1$ states, respectively.

Quantity \ Atom	F	Cl	Br	I
E_b	0.1250	0.1328	0.1236	0.1126
$\kappa^- - \kappa$	0.90	1.61	1.91	2.42
α	3.76	14.7	20.6	33.1
a/R	1.3	1.3	1.3	1.3
Z/Z_1	0.6	0.6	0.6	0.6

Z_l/Z_1, $l\neq 1$, to be approximately the same for these ions. Furthermore, we note that the major attractive interaction in the $l\neq 1$ state arises from the induced dipole and quadrupole terms. It is therefore not unreasonable to determine the ratios a/R and Z_l/Z_1, $l\neq 1$, by requiring that the integral over the region (R,∞) of the δ-function potential with weight functions 1 and r^{-1} is equal to the corresponding integral of the dipole and quadrupole potentials. This leads to

$$Z_l = \frac{\alpha}{6R^3} + \frac{\beta}{10R^5}, \quad l\neq 1 \tag{4.3}$$

$$Z_l/a = \frac{\alpha}{8R^4} + \frac{\beta}{12R^6}, \quad l\neq 1 \tag{4.4}$$

where α and β are dipolar and quadrupolar polarizabilities of the halogen atom. This implies that a/R is between 6/5 and 4/3 which are the values for very large β and very small β, respectively. We take an intermediate value

$$a/R = 1.3 \ . \tag{4.5}$$

A variation of this value between 1.2 and 1.4 does not significantly alter the results. We have also evaluated Z_l, $l\neq 1$, by using the values of α in Table I, and β given by Krishnagopal, Narasimhan, and Patil [18]. For example, with β equal to 85.0 for Cl and 125.0 for Br, we find that Z_l/Z_1, $l\neq 1$, is about 0.65 for Cl^- and 0.67 for Br^-. Since nonadiabatic effects tend to decrease the multipolar contributions, we take a slightly smaller value for the ratio:

$$Z \equiv Z_l, \quad l=0,2,3,\ldots$$
$$= 0.6 Z_1 \ . \tag{4.6}$$

In summary, a is determined in terms of R by Eq. (4.5), Z_l, $l\neq 1$ are determined in terms of Z_1 by Eq. (4.6), R is determined by Eq. (4.1), and Z_1 is determined by Eq. (4.2).

B. Polarizabilities

The contribution of the last electron to the dipolar polarizability of negative ions is given by

$$\alpha_1 = \tfrac{2}{3} \sum_{m_1=-1}^{1} \int \psi_b^{m_1}(\mathbf{r}) r\cos\theta \frac{1}{4\pi}[g_0(ib,r,r') + 5p_2(\hat{\mathbf{r}}\cdot\hat{\mathbf{r}}')g_2(ib,r,r')]r'\cos\theta'\psi_b^{m_1}(\mathbf{r}')dV\,dV'$$
$$= \tfrac{2}{9}\int_R^\infty \int_R^\infty \phi_b(r)[g_0(ib,r,r') + 2g_2(ib,r,r')]\phi_b(r')r^3 dr r'^3 dr' \ , \tag{4.7}$$

where $\phi_b(r)$ are given in Eq. (3.5) and $g_l(ib,r,r')$ are given in Eq. (2.16). To this α_1 we must add the polarizability of the neutral halogen atom to get the polarizability of the negative ion. The polarizabilities α of F, Cl, Br are those given by Miller and Bederson [19]. However, the value of α for I given by them appears to be small compared with other references. Therefore we take a slightly larger value of 33.1 given in Ref. [17]. The results for the total polarizabilities of negative halogen ions are given in Table II. The results are quite close to the larger of the values suggested by Coker [20]. We therefore feel that the predictions of our Green's functions are fairly reliable.

C. Multiphoton photodetachment cross sections

With the outgoing states normalized as in Eq. (3.16), the n-photon detachment cross section is

$$W_n = \frac{(2\pi)^{n+1}}{3} \frac{\hbar^{2n-3}(h\nu)^n}{a_B^n m^{n-1} c^n k} F^n \sum_{l,m_l} |M_{l,m_l}|^2 \ , \tag{4.8}$$

where

$$M = \sum_{i,j,\ldots} \frac{z_{fi}\cdots z_{jb}}{(E_i + E_b - nh\nu + h\nu)\cdots(E_j + E_b - h\nu)} \ , \tag{4.9}$$

a_B is the Bohr radius, ν is the frequency of the radiation, F is the photon flux, k is the momentum of the ejected electron,

$$k = [2m(nh\nu - E_b)/\hbar^2]^{1/2} \ , \tag{4.10}$$

and l, m_l are the angular momentum quantum numbers of the final state. In the matrix elements of M, the m_1 value of the initial state is equal to the m_l value of the final state. We write explicit expressions for M_{lm_l} for

TABLE II. Values of the hard-core radius R obtained from Eq. (4.1), Z_1 obtained from Eq. (4.2), and A_1 obtained from Eq. (3.7). Predictions for the dipolar polarizability α^- of the halogen ion in atomic units along with the larger of the values suggested by Coker [20], the two-photon detachment cross section $W_2(E_e)$ in cm^4 sec at $E_b=E_b/2$, and the scaled function $f_2(E_e/E_b)=W_2(E_e)/W_2(E_b/2)$.

Quantity \ Ion	F^-	Cl^-	Br^-	I
R	1.18	1.80	2.00	2.30
Z_1	1.92	1.34	1.22	1.09
A_1	0.909	0.852	0.795	0.726
α^-	14.2	35.7	48.1	74.1
	13.2[a]	33.8[a]	42.8[a]	65.9[a]
$W_2(E_b/2)$	2.33×10^{-50}	5.25×10^{-50}	7.75×10^{-50}	13.5×10^{-50}
$f_2(0.01)$	0.0282	0.0278	0.0277	0.0273
$f_2(0.04)$	0.184	0.177	0.175	0.171
$f_2(0.09)$	0.453	0.424	0.417	0.405
$f_2(0.16)$	0.723	0.666	0.653	0.632
$f_2(0.25)$	0.906	0.838	0.822	0.799
$f_2(0.36)$	0.989	0.938	0.926	0.908
$f_2(0.49)$	1.002	0.996	0.995	0.991
$f_2(0.64)$	0.984	1.052	1.066	1.090
$f_2(0.81)$	0.95	1.163	1.216	1.298

[a]Reference [20].

two-, three-, and four-photon detachment cross sections. For these cases, the elements are the same for $\pm m_l$.

For two-photon absorption, one has

$$M_{10}=\tfrac{1}{3}I_{10}+\tfrac{4}{15}I_{12}\ , \tag{4.11}$$

$$M_{11}=\tfrac{1}{5}I_{12}\ , \tag{4.12}$$

$$M_{30}=\left[\frac{12}{175}\right]^{1/2}I_{32}\ , \tag{4.13}$$

$$M_{31}=(\tfrac{2}{3})^{1/2}M_{30}\ , \tag{4.14}$$

with

$$I_{lj}=\int\phi_l(k,r)g_j(ib_1,r,r')\phi_b(r')r^3dr\,r'^3dr'\ , \tag{4.15}$$

where $\phi_l(k,r)$ are given in Eq. (3.12), $g_j(ib_1,r,r')$ is given in Eq. (2.16) with

$$b_1=[2m(E_b-h\nu)/\hbar^2]^{1/2}\ , \tag{4.16}$$

and $\phi_b(r')$ is given in Eq. (3.5).

For three-photon absorption, we have

$$M_{00}=(27)^{-1/2}(I_{010}+\tfrac{4}{5}I_{012})\ , \tag{4.17}$$

$$M_{20}=(15)^{-1/2}(\tfrac{2}{3}I_{210}+\tfrac{8}{15}I_{212}+\tfrac{18}{35}I_{232})\ , \tag{4.18}$$

$$M_{40}=\tfrac{8}{35}(3)^{-1/2}I_{432}\ , \tag{4.19}$$

$$M_{21}=(125)^{-1/2}(I_{212}+\tfrac{8}{7}I_{232})\ , \tag{4.20}$$

$$M_{41}=(\tfrac{5}{8})^{1/2}M_{40}\ , \tag{4.21}$$

where

$$I_{ljm}=\int\phi_l(k,r)g_j(ib_2,r,r')g_m(ib_1,r',r'')\phi_b(r'')\times r^3dr\,r'^3dr'r''^3dr''\ , \tag{4.22}$$

with

$$b_2=[2m(E_b-2h\nu)/\hbar^2]^{1/2}\ . \tag{4.23}$$

Finally, for the four-photon absorption, we have

$$M_{10}=\tfrac{1}{9}(\tfrac{4}{5}I_{1210}+I_{1010}+\tfrac{16}{25}I_{1212}+\tfrac{4}{5}I_{1012}+\tfrac{108}{175}I_{1232})\ , \tag{4.24}$$

$$M_{11}=\tfrac{1}{25}(I_{1212}+\tfrac{8}{7}I_{1232})\ , \tag{4.25}$$

$$M_{30}=(\tfrac{4}{525})^{1/2}(I_{3210}+\tfrac{4}{5}I_{3212}+\tfrac{16}{21}I_{3432}+\tfrac{27}{35}I_{3232})\ , \tag{4.26}$$

$$M_{31}=\tfrac{1}{25}(\tfrac{8}{7})^{1/2}(I_{3212}+\tfrac{25}{21}I_{3432}+\tfrac{8}{7}I_{3232})\ , \tag{4.27}$$

$$M_{50}=\tfrac{8}{21}(\tfrac{1}{33})^{1/2}I_{5432}\ , \tag{4.28}$$

$$M_{51}=(\tfrac{3}{5})^{1/2}M_{50}\ , \tag{4.29}$$

where

$$I_{ljmn}=\int\phi_l(k,r)g_j(ib_3,r,r')g_m(ib_2,r',r'')\times g_n(ib_1,r'',r''')\times\phi_b(r''')r^3dr\,r'^3dr'r''^3dr''r'''^3dr'''\ , \tag{4.30}$$

with

$$b_3=[2m(E_b-3h\nu)/\hbar^2]^{1/2}\ . \tag{4.31}$$

We do all our calculations in atomic units ($e=\hbar=m=1$, $c=137$), and multiply the n-photon detachment cross section by $4.139\times10^{16}\times(6.761\times10^{-34})^n$ to convert it into units of cm^{2n}sec^{n-1}. We have presented the results for the cross sections for some energies of the ejected electron, and also for relative amplitudes R_{lm_l},

$$R_{lm_l}=M_{lm_l}\Big/\left[\sum_{l,m_l}|M_{lm_l}|^2\right]^{1/2}\ . \tag{4.32}$$

TABLE III. Relative amplitudes $R_{lm_l}(E_e/E_b)$ for two-photon dissociation as functions of the scaled electron energy, E_e being the energy of the ejected electron and E_b being the electron affinity, where lm_l are the angular momentum quantum members of the final electron. The relative amplitude R_{31} equal to $(\frac{2}{3})^{1/2}R_{30}$.

Amplitude \ Ion	F^-	Cl^-	Br^-	I^-
$R_{10}(0.01)$	−0.960	−0.959	−0.959	−0.958
$R_{10}(0.09)$	−0.962	−0.960	−0.959	−0.959
$R_{10}(0.25)$	−0.955	−0.950	−0.949	−0.948
$R_{10}(0.49)$	−0.928	−0.919	−0.916	−0.914
$R_{10}(0.81)$	−0.89	−0.89	−0.89	−0.90
$R_{11}(0.01)$	−0.197	−0.201	−0.201	−0.202
$R_{11}(0.09)$	−0.188	−0.192	−0.193	−0.194
$R_{11}(0.25)$	−0.169	−0.173	−0.174	−0.174
$R_{11}(0.49)$	−0.138	−0.142	−0.143	−0.143
$R_{11}(0.81)$	−0.099	−0.101	−0.101	−0.100
$R_{30}(0.01)$	0.0044	0.0047	0.0048	0.0049
$R_{30}(0.09)$	0.0407	0.0448	0.0460	0.0472
$R_{30}(0.25)$	0.114	0.126	0.130	0.133
$R_{30}(0.49)$	0.207	0.222	0.227	0.230
$R_{30}(0.81)$	0.29	0.28	0.28	0.27

V. DISCUSSION

We now compare the predictions of our model with the experimental values and the results of other calculations, and point out some general properties of the cross sections.

A. Two-photon cross sections

Our predictions for two-photon cross sections and relative amplitudes are given in Tables II and III, and in Fig. 1. We find it convenient to present the results for the scaled cross section function

$$f_2(E_e/E_b)=W_2(E_e)/W_2(E_b/2) \tag{5.1}$$

and the relative amplitudes $R_{lm_l}(E_e/E_b)$, as functions of the scaled variable E_e/E_b, where E_e is the energy of the ejected electron and E_b is the electron affinity of the halogen atom.

Fluorine ion. Kwon *et al.* [6] have observed a value of $W_2=2.0(7)\times10^{-50}$ cm^{4}sec at $E_e=0.046\,32$ a.u. Our prediction at this energy is 2.3×10^{-50} cm^{4}sec. The central-potential model [4] gives a value of 4.3×10^{-50} cm^{4}sec, whereas the frozen-core, Hartree-Fock model [10] gives a value of 1.7×10^{-50} cm^{4}sec.

Chlorine ion. Trainham, Fletcher, and Larsen, [5] have observed a value of $W_2=1.3(9)\times10^{-50}$ cm^{4}sec at $E_e=4.78\times10^{-3}$ a.u. Our prediction at this energy is 0.9×10^{-50} cm^{4}sec whereas the prediction of the central-potential model is 1.68×10^{-50} cm^{4}sec. Recently, Jiang and Starace [11] have calculated the cross section with different approximations. Our predictions are in good agreement with their results, generally within 20%.

Bromine ion. Blondel *et al.* [8] have given various relative amplitudes at $h\nu=8.57\times10^{-2}$ a.u. Their values are

$$|R_{11}|=0.175 \text{ (calculated)}$$
$$=0.272 \text{ (measured)}, \tag{5.2}$$
$$|R_{30}|=0.08 \text{ (calculated)}$$
$$=0.106 \text{ (measured)}. \tag{5.3}$$

In comparing our predictions with these results, we must observe that these results are for the $P_{1/2}$ state of the electron. For this state, the threshold energy is 0.1420 a.u. With $2h\nu=0.1714$ a.u., we have $E_e/E_b=0.207$.

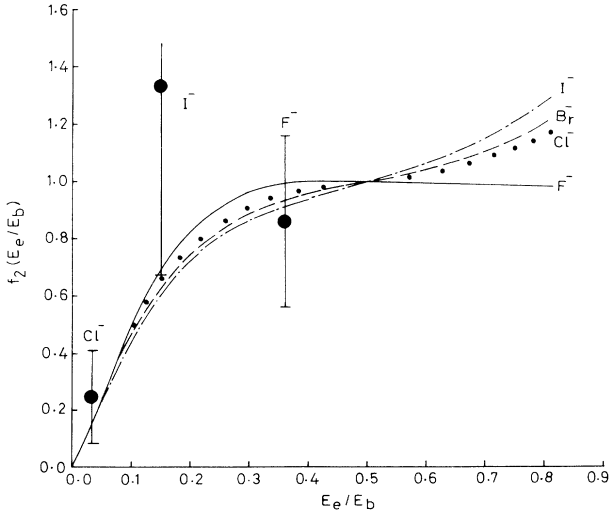

FIG. 1. Plot of the scaled two-photon cross section $f_2(E_e/E_b)=W_2(E_e)/W_2(E_b/2)$. E_e is the energy of the ejected electron and E_b is the electron affinity. —— is for F^-, · · · · for Cl^-, — — — for Br^-, and —·—·— for I^-. The experimental values are from Kwon *et al.* [6] for F^-, Trainham, Fletcher, and Larsen [5] for Cl^-, and Hall, Robinson, and Branscomb [3] for I^-.

TABLE IV. Three-photon detachment cross section $W_3(E_e)$ in $cm^6 sec^2$ at $E_e = E_b/4$, E_e being the energy of the ejected electron and E_b is electron affinity of the halogen atom, scaled function $f_3(2E_e/E_b) = W_3(E_e)/W_3(E_b/4)$, and the relative amplitude $R_{00}(2E_e/E_b)$ for the final electron state with $l=0$, $m=0$.

Quantity \ Ion	F^-	Cl^-	Br^-	I^-
$W_3(E_b/4)$	1.54×10^{-82}	3.30×10^{-82}	5.74×10^{-82}	12.4×10^{-82}
$f_3(0.01)$	0.519	0.533	0.536	0.586
$f_3(0.04)$	0.787	0.742	0.723	0.723
$f_3(0.09)$	0.774	0.638	0.593	0.523
$f_3(0.16)$	0.664	0.493	0.447	0.373
$f_3(0.25)$	0.652	0.528	0.503	0.467
$f_3(0.36)$	0.791	0.743	0.739	0.736
$f_3(0.49)$	0.993	0.994	0.993	0.991
$f_3(0.64)$	1.150	1.137	1.125	1.102
$f_3(0.81)$	1.250	1.103	1.090	1.024
$R_{00}(0.01)$	1.00	1.00	1.00	1.00
$R_{00}(0.09)$	0.946	0.936	0.931	0.924
$R_{00}(0.25)$	0.474	0.288	0.226	0.107
$R_{00}(0.49)$	−0.128	−0.283	−0.318	−0.367
$R_{00}(0.81)$	−0.406	−0.481	−0.501	−0.515

Since the relative amplitude depends primarily on the ratios of E_e/E_b, our predictions are (Table III)

$$|R_{11}| = 0.179 , \tag{5.4}$$

$$|R_{30}| = 0.107 . \tag{5.5}$$

These predictions agree quite well with the results of Blondel *et al.* [8].

Iodine ion. The two-photon cross section was observed by Hall, Robinson, and Branscomb [3] to be $W_2 = 1.8\times10^{-49}$ $cm^4 sec$ at $E_e = 0.0187$ a.u. However, this result has large error bars and suggests a value of $9\times10^{-50} < W_2 < 32\times10^{-50}$ $cm^4 sec$ as indicated by Crance [10]. It does not allow us to discriminate between different theoretical values. Our predictions given in Table II and Fig. 1 are lower than the results of Robinson and Geltman [4].

B. Three-photon cross sections

Our predictions for three-photon cross sections and relative amplitudes are given in Tables IV and V, and in Fig. 2. We have given the results for the scaled cross section

$$f_3(2E_e/E_b) = W_3(E_e)/W_3(E_b/4) \tag{5.6}$$

and the relative amplitudes $R_{lm_l}(2E_e/E_b)$ as functions of the scaled variable $2E_e/E_b$.

Fluorine ion. Here there are two experimental observations. Blondel *et al.* [7] have observed a value of

TABLE V. Relative amplitude $R_{lm_l}(2E_e/E_b)$ for three-photon dissociation as functions of the scaled electron energy, E_e being the energy of the ejected electron and E_b being the electron affinity, and lm_l are the angular momentum quantum numbers of the final electron. The ratio R_{41} is equal to $(\frac{5}{8})^{1/2}R_{40}$.

Amplitude \ Ion	F^-	Cl^-	Br^-	I^-
$R_{20}(0.01)$	0.028	0.028	0.027	0.026
$R_{20}(0.09)$	0.300	0.325	0.335	0.353
$R_{20}(0.25)$	0.818	0.887	0.901	0.919
$R_{20}(0.49)$	0.924	0.888	0.877	0.859
$R_{20}(0.81)$	0.846	0.800	0.787	0.776
$R_{21}(0.01)$	0.008	0.008	0.008	0.008
$R_{21}(0.09)$	0.087	0.096	0.100	0.105
$R_{21}(0.25)$	0.227	0.252	0.258	0.264
$R_{21}(0.49)$	0.238	0.237	0.236	0.233
$R_{21}(0.81)$	0.195	0.195	0.195	0.195
$R_{40}(0.01)$	5.1×10^{-5}	5.1×10^{-5}	5.1×10^{-5}	4.8×10^{-5}
$R_{40}(0.09)$	0.0049	0.0055	0.0057	0.0060
$R_{40}(0.25)$	0.038	0.043	0.044	0.045
$R_{40}(0.49)$	0.087	0.089	0.090	0.090
$R_{40}(0.81)$	0.137	0.152	0.154	0.158

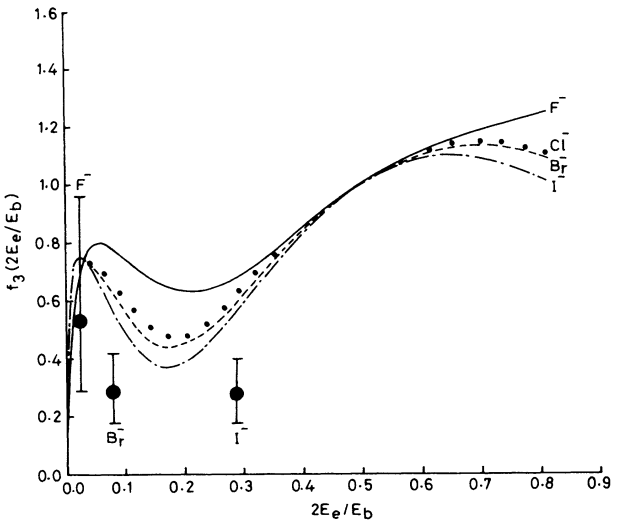

FIG. 2. Plot of the scaled three-photon cross section $f_3(2E_e/E_b)=W_3(E_e)/W_3(E_b/4)$, E_e being the energy of the ejected electron and E_b is the electron affinity. —— is for F^-, · · · · for Cl^-, — — — for Br^-, and —·—·— for I^-. The experimental values are from Kwon *et al.* [6] for F^-, and Blondel *et al.* [7] for Br^- and I^-.

$W_3=(0.61^{+0.26}_{-0.18})\times10^{-82}$ cm^{6}sec^2 at $E_\gamma=4.283\times10^{-2}$ a.u. At the same energy, Kwon *et al.* [6] have reported a value of $(0.79^{+0.66}_{-0.36})\times10^{-82}$ cm^{6}sec^2. Our prediction at this energy is 1.2×10^{-82} cm^{6}sec^2. Theoretical calculations of Crance [10] give results which range between $(0.6-1.0)\times10^{-82}$ cm^{6}sec^2. The agreement between different results is quite satisfactory.

Chlorine ion. Our values for the cross sections are smaller than the predictions of Crance [10]. For example, at $E_e=0.01$ a.u., our cross section is $W_3=1.65\times10^{-82}$ cm^{6}sec^2, whereas the value of Crance is about 3×10^{-82} cm^{6}sec^2.

Bromine ion. Blondel *et al.* [7] have observed a value of $W_3=(1.6^{+0.8}_{-0.6})\times10^{-82}$ cm^{6}sec^2 at $E_\gamma=4.283\times10^{-2}$ a.u. Our prediction at this energy is 3.6×10^{-82} cm^{6}sec^2, whereas the prediction of Crance [10] is 5.9×10^{-82} cm^{6}sec^2. Blondel *et al.* [8] have also given the values for some relative amplitudes at $E_e=4.78\times10^{-3}$ a.u. Their values are

$$|R_{20}|=0.208 \text{ (calculated)}$$
$$=0.118 \text{ (measured)}, \tag{5.7}$$
$$|R_{21}|=0.053 \text{ (calculated)}$$
$$=0.091 \text{ (measured)}. \tag{5.8}$$

Our predictions at the energy are

$$|R_{20}|=0.29, \tag{5.9}$$
$$|R_{21}|=0.087. \tag{5.10}$$

Iodine ion. Blondel *et al.* [7] have observed a value of $W_3=(3.3^{+1.6}_{-1.6})\times10^{-82}$ cm^{6}sec^2 at $E_\gamma=4.283\times10^{-2}$ a.u. Our prediction is 6.7×10^{-82} cm^{6}sec^2, whereas that of Crance [10] is 14×10^{-82} cm^{6}sec^2.

C. Four-photon cross sections

Our predictions for four-photon cross sections and relative amplitudes are given in Tables VI and VII, and in Fig. 3. We have given the results for the scaled cross section

$$f_4(3E_e/E_b)=W_4(E_e)/W_4(E_b/6) \tag{5.11}$$

and relative amplitude $R_{lm_l}(3E_e/E_b)$ as functions of the scaled variable $3E_e/E_b$.

Experimentally, Blondel and Trainham [9] have ob-

TABLE VI. Four-photon detachment cross section $W_4(E_e)$ in cm^{8}sec^3 at $E_e=E_b/6$, E_e being the energy of the ejected electron and E_b is the electron affinity of the halogen atom, scaled function $f_4(3E_e/E_b)=W_4(E_e)/W_4(E_b/6)$, and relative amplitude $R_{10}(3E_e/E_b)$ for the final electron state with $l=1, m=0$.

Quantity \ Ion	F^-	Cl^-	Br^-	I^-
$W_4(E_b/6)$	2.40×10^{-114}	4.28×10^{-114}	8.38×10^{-114}	21.3×10^{-114}
$f_4(0.01)$	0.047	0.045	0.045	0.045
$f_4(0.04)$	0.310	0.297	0.297	0.294
$f_4(0.09)$	0.758	0.722	0.720	0.710
$f_4(0.16)$	1.157	1.098	1.091	1.075
$f_4(0.25)$	1.313	1.248	1.238	1.222
$f_4(0.36)$	1.221	1.176	1.169	1.158
$f_4(0.49)$	1.010	1.009	1.008	1.007
$f_4(0.64)$	0.852	0.867	0.873	0.879
$f_4(0.81)$	0.760	0.803	0.808	0.813
$R_{10}(0.01)$	−0.987	−0.986	−0.986	−0.986
$R_{10}(0.09)$	−0.984	−0.983	−0.983	−0.983
$R_{10}(0.25)$	−0.953	−0.949	−0.948	−0.947
$R_{10}(0.49)$	−0.784	−0.773	−0.769	−0.768
$R_{10}(0.64)$	−0.585	−0.581	−0.576	−0.581

TABLE VII. Relative amplitudes $R_{lm}(3E_e/E_b)$ for three-photon dissociation, as functions of the scaled electron energy, E_e being the energy of the ejected electron and E_b being the electron affinity, where lm are the angular momentum quantum numbers of the final electron. The relative amplitude R_{51} is $(\frac{3}{5})^{1/2}R_{50}$.

Amplitude \ Ion	F^-	Cl^-	Br^-	I^-
$R_{11}(0.01)$	−0.115	−0.118	−0.119	−0.119
$R_{11}(0.09)$	−0.110	−0.114	−0.115	−0.116
$R_{11}(0.25)$	−0.097	−0.102	−0.103	−0.104
$R_{11}(0.49)$	−0.062	−0.068	−0.069	−0.070
$R_{11}(0.64)$	−0.032	−0.038	−0.040	−0.041
$R_{30}(0.01)$	0.0077	0.0078	0.0079	0.0079
$R_{30}(0.09)$	0.075	0.077	0.078	0.078
$R_{30}(0.25)$	0.243	0.251	0.254	0.256
$R_{30}(0.49)$	0.556	0.565	0.569	0.569
$R_{30}(0.64)$	0.735	0.734	0.736	0.732
$R_{31}(0.01)$	0.0028	0.0028	0.0029	0.0029
$R_{31}(0.09)$	0.027	0.027	0.028	0.028
$R_{31}(0.25)$	0.084	0.087	0.089	0.090
$R_{31}(0.49)$	0.183	0.189	0.192	0.193
$R_{31}(0.64)$	0.235	0.240	0.242	0.242
$R_{50}(0.01)$	8.0×10^{-6}	8.0×10^{-6}	8.1×10^{-6}	8.2×10^{-6}
$R_{50}(0.09)$	7.1×10^{-4}	7.2×10^{-4}	7.3×10^{-4}	7.4×10^{-4}
$R_{50}(0.25)$	0.0065	0.0067	0.0068	0.0069
$R_{50}(0.49)$	0.0297	0.0304	0.0309	0.311
$R_{50}(0.64)$	0.0519	0.0529	0.0536	0.0536

served $W_4=(9.8^{+6.9}_{-4.1})\times10^{-115}$ cm^8 sec^3 at $E_\gamma=4.283\times10^{-2}$ a.u. for Cl^-. Our prediction is 33.0×10^{-115} cm^8 sec^3, whereas that of Crance [10] is 46×10^{-115} cm^8 sec^3.

D. Some general trends

Our model is sufficiently simple that one can analyze the trends in the cross sections and relative amplitudes.

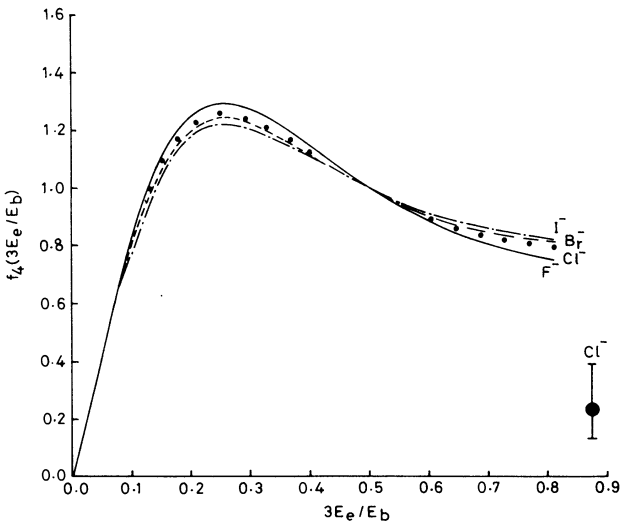

FIG. 3. Plot of the scaled four-photon cross section $f_4(3E_e/E_b)=W_4(E_e)/W_4(E_b/6)$. E_e is the energy of the ejected electron and E_b is the electron affinity. —— is for F^-, · · · · for Cl^-, — — — for Br^-, and —·—·— for I^-. The experimental value for Cl^- is from Blondel and Trainham [9].

These trends show some important similarities and some differences for different halogen ions.

To start with, we note that the Green's function in Eq. (2.16) has a pole at k given by the condition

$$1-g_l^{(0)}(k,a,a)Z_l a^2=0, \quad l\neq1 . \tag{5.12}$$

The critical value of Z_l at which the pole begins to appear as a bound state is given by

$$Z_l=\frac{1}{a^2 g_l^{(0)}(0,a,a)} =\frac{2l+1}{2a}[1-(R/a)^{2l+1}]^{-1} . \tag{5.13}$$

The value of $Z=Z_l$, $l\neq1$, we have chosen (Table I) is less than this value. However, the complex k at which the pole given in Eq. (5.12) appears approaches the origin as we progress from F^- to I^-, particularly for $l=0$. This is the main reason why our two-photon cross section W_2 near $E_e\approx E_b$ shows an increasingly upward trend (Fig. 1) as we go from F^- to I^-. Of course, one does expect a resonance pole to exist. The important question is, how close is it to $k=0$, and whether its effect is sufficiently large to produce a noticeable upturn near $E_e\approx E_b$.

The resonance effect is quite obvious in the three-photon cross sections W_3 (Fig. 2). It is observed that the resonance moves closer to $E_e=0$ and becomes sharper as we go from F^- to I^-. There is also a dip in the cross sections at $E_e\approx(0.08\text{–}0.11)E_b$, and there may be a second maximum near $E_e\approx0.33E_b$.

The scaled four-photon cross sections as functions of the scaled variable $3E_e/E_b$ show a universal form (Fig. 3) with little variation as we go from F^- to I^-. There is a

maximum in $W_4(E_e)$ near $E_e \approx 0.08 E_b$.

In some ways, the most striking feature of our results is the near equality of the different relative amplitudes R_{lm_l} as functions of the scaled variable $(n-1)E_e/E_b$, n is the number of photons, for the different halogen ions (Tables III–VII). An interesting point here is that for the three-photon detachment cross sections, R_{00} changes its sign at $E_e \approx (0.17 \pm 0.03) E_b$.

Before concluding, we assess the dependence of the results on the various input parameters. As noted earlier, the results are fairly insensitive to a variation of the ratio a/R between 1.2 and 1.4. The hard-core radius R is determined primarily by the contribution of the last electron to the diamagnetic susceptibility as in Eq. (4.1), and R changes by only about 5% when the susceptibility is varied by 10%. The strength Z_1 of the δ-function potential in the $l=1$ state is related to the electron affinity as in Eq. (4.2). Since the electron affinities are known quite accurately [21], for a given value of R, there is little freedom in the choice of Z_1. The major uncertainties in our results are due to the choice of the values of Z given in Eq. (4.6). Though the values we have chosen in Eq. (4.6) are reasonable, we cannot rule out a value which is smaller by about 20%. With a smaller value of Z/Z_1, the various cross sections are somewhat smaller, the resonance pole moves farther away from the real axis, and the resonance effects will be less prominent, that is, the upturn of the two-photon cross sections will be less pronounced and the rise in the three-photon cross sections will be less sharp. Regarding our suggestion that the resonance may approach the real axis as we go from F^- to I^-, while it is a consequence of the approximation we have made in Eq. (4.6), we also think that it is physically reasonable. In this connection, we mention an interesting observation that a negative ion with the last electron outside the closed shell has been found [22] for Ca^- with an electron affinity of 0.043 ± 0.007 eV, but not for the lighter alkaline-earth-metal ion Mg^-.

VI. CONCLUSIONS

We have presented a simple model for the polarizabilities of negative halogen ions and their multiphoton-detachment cross sections. It is based on wave functions and Green's functions for δ-function potentials with a hard core. The hard core is intended to simulate the short-range exchange repulsion. This is similar in spirit to the $1/r^2$ repulsive term used by Adelman and Szabo [23] in the analysis of polarizabilities of alkali-metal atoms. The advantages of this model are that it is sufficiently simple as to allow us to observe certain trends in the cross sections and the amplitudes. However, though the model is very simple, we must emphasize that strong constraints are placed on the predictions by the inputs of electron affinities, diagmagnetic susceptibilities, and polarizabilities of halogen atoms. A fairly good prediction of the polarizabilities of negative halogen ions is an indication of the reliability of the model.

There are some striking features of the predictions of our analysis. There is a pole in the Green's function at a complex k which approaches $k=0$ as we progress from F^- to I^-. This gives rise to a resonant behavior in the three-photon cross sections W_3 near $E_e \approx 0$. It also gives rise to an increasing upturn of the two-photon cross sections near $E_e \approx E_b$. Another important feature is that the relative amplitudes R_{lm_l} as functions of the scaled variable $(n-1)E_e/E_b$ are approximately the same for all halogens. It would be very interesting if future experiments confirm these predictions.

ACKNOWLEDGMENTS

I thank Mr. B. A. Bapat for verifying the results for polarizabilities and two-photon cross sections.

[1] P. Hammerling (unpublished).
[2] S. Geltman, Phys. Lett. **4**, 168 (1963); **19**, 616 (1965).
[3] J. L. Hall, E. J. Robinson, and L. M. Branscomb, Phys. Rev. Lett. **14**, 1013 (1965).
[4] E. J. Robinson and S. Geltman, Phys. Rev. **153**, 4 (1967).
[5] R. Trainham, G. D. Fletcher, and D. J. Larsen, J. Phys. B **20**, L777 (1987).
[6] N. Kwon, P. S. Armstrong, T. Olsson, R. Trainham, and D. J. Larsen, Phys. Rev. A **40**, 676 (1989).
[7] C. Blondel, R. J. Champeau, M. Crance, A. Crubellier, D. Delsart, and D. Marinescu, J. Phys. B **22**, 1335 (1989).
[8] C. Blondel, M. Crance, C. Delsart, A. Girourd, and R. Trainham, J. Phys. B **23**, L685 (1990).
[9] C. Blondel and R. Trainham, J. Opt. Soc. Am. B **6**, 1774 (1989).
[10] M. Crance, J. Phys. B **20**, 6553 (1987); **20**, L411 (1987); **21**, 3559 (1988).
[11] T. F. Jiang and A. F. Starace, Phys. Rev. A **38**, 2347 (1988).
[12] C. Pan, B. Gao, and E. F. Starace, Phys. Rev. A **41**, 6271 (1990); C. Pan and A. F. Starace, *ibid.* **44**, 324 (1991); A. L'Huillier and G. Wendin, J. Phys. B **21**, L247 (1988); P. A. Golovinsky, I. Yu Kian, and V. S. Rostovtsev, *ibid.* **23**, 2743 (1990).
[13] J. Meixner, Math. Z. **36**, 677 (1933); H. F. Hameka, J. Chem. Phys. **47**, 2728 (1967).
[14] A. Declemy, A. Rachman, M. Jaouen, and G. Laplanche, Phys. Rev. A **23**, 1823 (1981).
[15] G. Malli and S. Fraga, Theor. Chim. Acta **5**, 284 (1966).
[16] J. C. Slater, Phys. Rev. **32**, 349 (1928); **36**, 57 (1930); G. W. Brindley, Philos. Mag. **11**, 786 (1931).
[17] S. H. Patil, J. Chem. Phys. **83**, 5764 (1985).
[18] S. Krishnagopal, S. Narasimhan, and S. H. Patil, J. Chem. Phys. **83**, 5772 (1985).
[19] T. M. Miller and B. Bederson, Adv. At. Mol. Phys. **13**, 1 (1977).
[20] H. Coker, J. Phys. Chem. **80**, 2078 (1976).
[21] *CRC Handbook of Chemistry and Physics,* 71st ed. (CRC, Boca Raton, 1990).
[22] D. J. Pegg, J. S. Thompson, R. M. Compton, and G. D. Alton, Phys. Rev. Lett. **59**, 2267 (1987).
[23] S. A. Adelman and A. Szabo, J. Chem. Phys. **58**, 687 (1973).